A compact 24 GHz quadrature Doppler radar with front-end MMIC

Choul-Young Kim [a] & Songcheol Hong [b c]

[a] Electronics Engineering, Chungnam National University ,
Daejeon , Republic of Korea

[b] Department of Electrical Engineering , Korea Advanced Institute
of Science and Technology , Daejeon , Republic of Korea

[c] Department of and Computer Science , Korea Advanced Institute
of Science and Technology , Daejeon , Republic of Korea
Published online: 06 Dec 2012.

PLEASE SCROLL DOWN FOR ARTICLE

Taylor & Francis
Taylor & Francis Group

A compact 24 GHz quadrature Doppler radar with front-end MMIC

Choul-Young Kim[a]* and Songcheol Hong[bc]

[a]*Electronics Engineering, Chungnam National University, Daejeon, Republic of Korea;*
[b]*Department of Electrical Engineering, Korea Advanced Institute of Science and Technology,
Daejeon, Republic of Korea;* [c]*Department of and Computer Science, Korea Advanced
Institute of Science and Technology, Daejeon, Republic of Korea*

A compact 24 GHz quadrature Doppler radar front-end monolithic microwave integrated circuit (MMIC) with Tx leakage canceller is developed. The chip is $3 \times 2 \, mm^2$ and the front-end module is $3 \times 3 \, cm^2$. The MMIC consists of a 24 GHz voltage-controlled oscillator, a Tx leakage canceller and two mixers. The radar module can measure speeds as low as 2.5 mm/s, which corresponds to a 0.41 Hz Doppler shift. The quadrature topology enables the signs of a Doppler shift to be detected and obviates the null point problems.

Keywords: GaAs MMIC; microwave sensors; RF front-ends; velocity; Doppler radar

1. Introduction

Microwave and millimetre-wave Doppler radar have gained considerable attention in various applications such as automotive safety systems, ubiquitous healthcare systems and human motion detection systems (Meinel 1995). For these commercial applications, high performance, compact size and low-cost requirements are crucial (Klotz and Rohling 2001; Russel, Drubin, Marinilli, Woodington, and Del Checcolo 2002).

Continuous wave (CW) radars with a single antenna are based on very simple structures that allow small-size and low-cost solutions. In CW radar systems such as FMCW radars or Doppler radars, a high Tx-to-Rx isolation is required to improve sensitivity (Skolnik 1980). The Tx leakage canceller provides a higher level of Tx-to-Rx isolation than a single Lange coupler and has wideband characteristics. A Tx leakage canceller was implemented in a Doppler radar with a branch-line hybrid coupler (Kim, Kim, and Hong 2007). However, the size of the radar module is relatively large ($5 \times 7 \, cm^2$) due to the size of the branch-line couplers. An interferometer can be configured to measure the displacement and velocity. Quadrature Doppler radar can detect the speed and direction of a target and act as an interferometer to measure the displacement (Kim and Nguyen 2003, 2004); it also obviates null point problems during the measurement process (Droitcour, Lubecke, Lubecke, Lin, and Kovacs 2004). Recently, Doppler radar with the quadrature hybrid mixer was also proposed to improve the power loss in transmit and receive paths (Ho and Chung 2010). Front-end integrated circuits for Doppler radars or FMCW radars also have been demonstrated using CMOS and BiCMOS technology

---

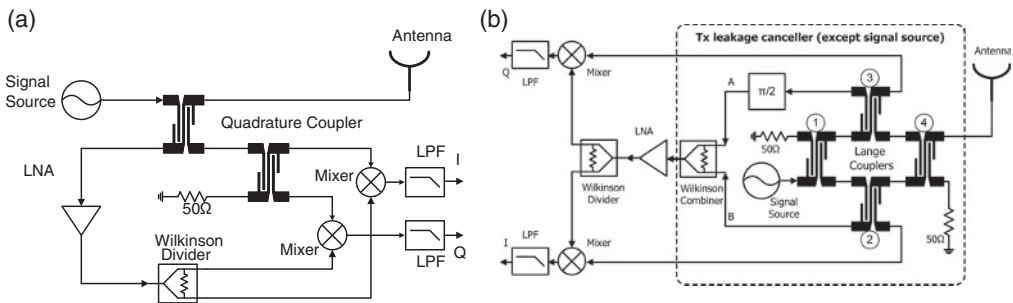*Corresponding author. Email: cykim@cnu.ac.kr

Figure 1. Block diagrams of: (a) a quadrature radar without a Tx leakage canceller and (b) a quadrature radar with a Tx leakage canceller.

(Chen, Hsieh, and Lu 2008; Nicolson, Chevalier, Sautreuil, and Voinigescu 2008). However, the all demonstrated front-end ICs are for two antenna systems. Thus, the overall size of front-end module including two antennas for transmitting and receiving is inevitably large.

In this study, we present a compact 24 GHz quadrature Doppler radar with front-end monolithic microwave integrated circuit (MMIC) which has a Tx leakage canceller. MMIC technologies are a key to compact size and low-cost manufacturing of high-performance radar systems. As mentioned before, the Tx leakage canceller with branch-line hybrid couplers on printed circuit board is relatively large. Therefore, the MMIC technologies are used for compact front-end module. For compact chip size, we designed bent Lange couplers and a compact Wilkinson combiner. The degraded coupling factor of the bent Lange coupler is explained in terms of even and odd mode current distributions. The size of the designed quadrature radar front-end module is $3 \times 3\,\mathrm{cm}^2$, which is about 75% smaller than a similar module in a previous work (Kim et al. 2007). This radar can measure speeds as low as 2.5 mm/s, which corresponds to a 0.41 Hz Doppler shift. The quadrature topology also enables it to detect signs of a Doppler shift. Moreover, it can measure the displacement of a target using proper signal processing like that used in Kim and Nguyen (2004).

2. MMIC design and measurement results

Figure 1 shows block diagrams of quadrature radars. The conventional quadrature radar shown in Figure 1(a) has two Lange couplers. One of the couplers separates the transmitting path and the receiving path. The other coupler provides LO signals for quadrature mixing. There is only a 3 dB loss in the receiving path. There are significant Tx leakage problems if the Lange coupler has low isolation. The quadrature radar shown in Figure 1(b) has a Tx leakage canceller to overcome the low isolation of the Lange coupler itself. The Tx leakage canceller is composed of four Lange couplers, a 90° delay line and a Wilkinson combiner. The Tx leakage canceller can provide higher Tx-to-Rx isolation than a Lange coupler. As shown in Figure 1(b), there is also only a 3 dB loss in the receiving path, as was the case with the quadrature radar without Tx leakage canceller.

2.1. *The effect of port mismatch in Tx leakage canceller*

The isolation characteristic of signal source port to canceller output port considering only the mismatches between two leakage paths through couplers 2 and 3 is shown in the previous work (Kim et al. 2007). In this study, we analyse on the effect of mismatch at any port of cancellers. In Tx leakage canceller, mismatches of an antenna port and two mixer ports affect the isolation characteristic. Thus, two reflected signals at the two input ports of the Wilkinson combiner because of mismatches at the two ports of mixers are shown as

$$V_{M\_L} = A_M \cdot \cos(\omega_T t + \phi_M) \tag{1}$$

$$V_{M\_R} = -(A_M + \Delta A_M) \cdot \cos(\omega_T t + \phi_M + \Delta\phi_M) \tag{2}$$

where V_{M_L} and V_{M_R} are the input signals of the Wilkinson combiner, A_M and ΔA_M are the amplitude of V_{M_L} and the amplitude mismatch of V_{M_R}, respectively, and ϕ_M and $\Delta\phi_M$ are the phase of V_{M_L} and the phase mismatch of V_{M_R}, respectively. Similarly, two reflected signals at the two input ports of the Wilkinson combiner because of mismatches at the antenna port are shown as

$$V_{A\_L} = A_A \cdot \cos(\omega_T t + \phi_A) \tag{3}$$

$$V_{A\_R} = (A_A + \Delta A_A) \cdot \cos(\omega_T t + \phi_A + \Delta\phi_A) \tag{4}$$

where V_{A_L} and V_{A_R} are the input signals of the Wilkinson combiner, A_A and ΔA_A are the amplitude of V_{A_L} and the amplitude mismatch of V_{A_R}, respectively, and ϕ_A and $\Delta\phi_A$ are the phase of V_{A_L} and the phase mismatch of V_{A_R}, respectively. The leakage signals at the output port of the Wilkinson combiner including the reflected signals due to mismatches at the ports are given as follows:

$$
\begin{aligned}
V_{Wil\_leakage} = {} & \frac{1}{\sqrt{2}} \cdot [A_L - (A_L + \Delta A_L)] \\
& \cdot \cos(\Delta\phi_L) \cdot \cos(\omega_T t + \phi_L - \beta_L) \\
& + \frac{1}{\sqrt{2}} \cdot [A_M - (A_M + \Delta A_M)] \\
& \cdot \cos(\Delta\phi_M) \cdot \cos(\omega_T t + \phi_M - \beta_M) \\
& + \frac{1}{\sqrt{2}} \cdot [A_A + (A_A + \Delta A_A)] \\
& \cdot \cos(\Delta\phi_A) \cdot \cos(\omega_T t + \phi_A - \beta_A)
\end{aligned}
\tag{5}
$$

where A_L and ΔA_L are the amplitude of one of the leakage signals through couplers 2 and 3 at the Wilkinson combiner input and the amplitude mismatch of two leakage signal, respectively, and ϕ_L and $\Delta\phi_L$ are the phase of leakage signal and the phase mismatch of two leakage signal, respectively, and

$$\tan\beta_{L,M} = \frac{(A_{L,M} + \Delta A_{L,M}) \cdot \sin(\Delta\phi_{L,M})}{A_{L,M} - (A_{L,M} + \Delta A_{L,M}) \cdot \cos(\Delta\phi_{L,M})}, \tag{6}$$

$$\tan\beta_A = \frac{-(A_A + \Delta A_A) \cdot \sin(\Delta\phi_A)}{A_A + (A_A + \Delta A_A) \cdot \cos(\Delta\phi_A)}. \tag{7}$$

If the amplitude and the phase mismatch between two reflected signals at the two mixer ports are very small, there is little influence of mismatch at the two mixer ports. The two reflected signals due to mismatch at antenna port also appear at the output port of the Wilkinson combiner. Although there is no amplitude and phase mismatch, the leakage signal due to mismatch at antenna port appear because they are in-phase. Therefore, low antenna port mismatch is necessary.

The isolation of single coupler and return losses at mixer and antenna port are described as

$$Iso_{coupler} = \frac{\sqrt{2}A_L}{A_T} \tag{8}$$

$$RL_{mixer} = \frac{2\sqrt{2}A_M}{A_T} \tag{9}$$

$$RL_{antenna} = \frac{2\sqrt{2}A_A}{A_T} \tag{10}$$

where A_T is the amplitude of the transmitted signal. Using Equations (1)–(10), the isolation of the Tx leakage canceller $Iso_{canceller}$ is described as

$$Iso_{canceller} = \left| \begin{array}{c} \frac{1}{2} \cdot Iso_{coupler} \cdot \left[1 - \left(1 + \frac{\Delta A_L}{A_L} \right) \right] \\ \cdot \cos(\Delta\phi_L) \cdot \cos(\omega_T t + \phi_L - \beta_L) \\ + \frac{1}{4} \cdot RL_{mixer} \cdot \left[1 - \left(1 + \frac{\Delta A_M}{A_M} \right) \right] \\ \cdot \cos(\Delta\phi_M) \cdot \cos(\omega_T t + \phi_M - \beta_M) \\ + \frac{1}{4} \cdot RL_{antenna} \cdot \left[1 + \left(1 + \frac{\Delta A_A}{A_A} \right) \right] \\ \cdot \cos(\Delta\phi_A) \cdot \cos(\omega_T t + \phi_A - \beta_A) \end{array} \right|. \tag{11}$$

The isolation of canceller depends on the symmetry of two paths, single coupler isolation and mismatch at mixers and antenna ports. Figure 2 shows the simulation results of the canceller isolation for different return loss conditions, 0, 0.1 and 0.2, at two mixers versus return loss difference between two mixers. As the simulations shown in Equation (11), canceller isolation is the more affected return loss difference between two mixers than return loss itself at two mixers.

2.2. *MMIC versus PCB hybrid technology for quadrature Doppler radar front-end with Tx leakage canceller*

As mentioned before, high performance, compact size and low cost are very important for commercial radar applications. The quadrature Doppler radar using branch-line hybrid couplers on printed circuit board using the hybrid technology is relatively large because passive components such as a branch-line hybrid coupler, a 90° delay line and a Wilkinson combiner are large. Therefore, quadrature radar front-end module using the hybrid technology is inevitably large. As presented in Table 1, the size of $\lambda/4$ line on the RO3003 PCB is 16 times larger than that on the GaAs substrate. In the cases of quadrature coupler and Wilkinson combiner, the size on the RO3003 PCB is 59 times and 122 times larger
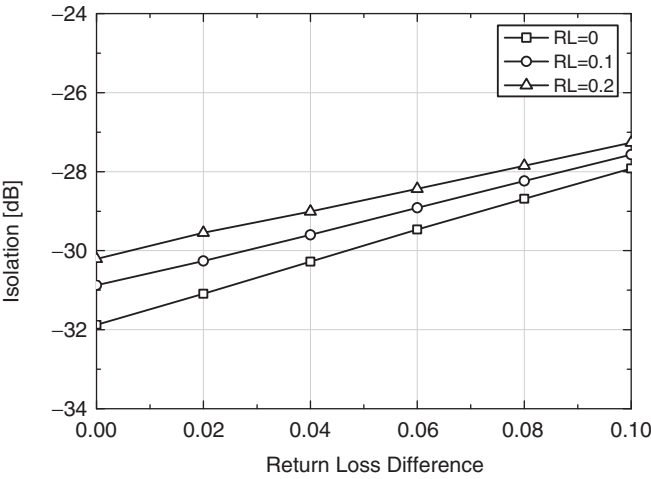
Figure 2. Simulation results of the canceller isolation for different return loss conditions at two mixers versus return loss difference between two mixers.

Table 1. Size comparison of passive components.

	$\lambda/4$ Line (mm)	Quadrature coupler (mm)	Wilkinson combiner (mm)
PCB (RO3003, $\varepsilon_r = 3$, thickness $= 256\,\mu m$) [Kim et al. 2007]	0.62×2	2.8×3.4 (branch-line hybrid)	2.9×3.4
Si MMIC (SiO$_2$, $\varepsilon_r = 4$, thickness $= 10\,\mu m$) [Chirala and Cam Nguyen 2006]	0.03×1.24	0.21×0.18 (Unfolded Lange)	N.A
GaAs MMIC (GaAs, $\varepsilon_r = 12.9$, thickness $= 100\,\mu m$) [this study]	0.07×1.1	0.13×1.24 (Lange)	0.23×0.35

than that on the GaAs substrate, respectively. For compact front-end, using MMIC technology is the best choice because the effective wavelength is small and compact quadrature coupler, Lange coupler and compact Wilkinson combiner are available as presented in Table 1. Lange couplers are the most widely used as they can be integrated into an MMIC. A Lange coupler is very compact compared to a branch-line hybrid coupler. A quadrature radar front-end circuit, as shown in Figure 1(a), has poor performance because the Lange coupler has low isolation although it is compact. Figure 1(b) shows the quadrature radar front-end circuit with Tx leakage canceller. The size of Wilkinson combiner could be reduced using another circuit topology with the MMIC technology. For high performance with compact size, Tx leakage canceller using the Lange coupler was implemented. As mentioned before, using Figure 2 and Equation (10), canceller isolation is more affected return loss balance between two mixers than each mixer's return loss itself. Therefore, the MMIC technology is more appropriate for high

isolation performance than the PCB hybrid technology because the MMIC technology is a more precision process than the PCB hybrid technology. Because the quadrature radar with the Tx leakage canceller requires two additional Lange couplers, a 90° delay line and a Wilkinson combiner, the chip of the quadrature radar might be quite large although they are much smaller than that made with the PCB hybrid technology.

2.3. *Silicon technology for quadrature Doppler radar front-end with Tx leakage canceller*

A branch-line hybrid coupler is not suitable for MMIC implementation because the size of the coupler is prohibitively large owing to the use of four quarter-wavelength transmission line. Although using the active inductor the compact branch-line hybrid coupler using the CMOS technology has been demonstrated at 4.2 GHz, it consumes power and it is still large (Hsieh, Liao, and Lu 2007). Lange coupler is more appropriate because it occupies small chip areas. The compact Lange coupler has been implemented in the monolithic silicon technology (Chirala and Nguyen 2006). As presented in Table 1, the size of the 90° delay line and unfolded Lange coupler are smaller than that the Lange coupler in the monolithic GaAs technology. However, the -12 dB isolation of the unfolded Lange coupler in the silicon technology is not suitable for a single antenna Doppler radar front-end topology because it results in the isolation problem between the transmit and receive paths.

2.4. *MMIC design*

To verify the operation of the Tx leakage canceller and the quadrature radar topology, we used a 6 inch InGaP/GaAs heterojunction bipolar transistor (HBT) foundry to design and fabricate the test structure of the Tx leakage canceller and the quadrature Doppler radar front-end MMIC, as shown in Figure 1(b). The technology provides a SiNx MIM capacitor with 600 pF/mm^2, a 50 $\Omega/\square$ NiCr resistor and two metal layers with a thickness of 1.3 and 4 μm, respectively. All circuits are passivated by polymide. All the passive components, namely the Lange couplers, the microstrip delay line and the Wilkinson combiner, were designed with a 2.5D EM simulator. The Lange couplers are the most widely used because they can be integrated into an MMIC. In the Tx leakage canceller, the two Lange couplers (couplers 2 and 3) are bent to reduce the overall chip size. The bending of the microstrip line can degrade the circuit performance. Such discontinuities generate several problems: for instance, a reactive effect that causes a reflection, a current crowding effect that causes an increasing resistance and radiation of the microwave signal. In conclusion, the bending of the microstrip introduces a loss.

As shown in Figure 3(a), we used the improved lumped-distributed Wilkinson combiner topology, which is demonstrated at 1.8 GHz on an FR4 substrate (Chongcheawchamnan, Siripon, and Robertson 2001). The circuit uses only one via-ground for a shunted input capacitor, thereby minimising the parasitic effects and making the circuit smaller overall. The designed circuit of a conventional topology is about 350×600 μm^2. However, the designed circuit shown in Figure 3(b) is about 230×350 μm^2, which is about 2.6 times smaller than a conventional circuit. The microstrip line is used for a delay line. We also designed a voltage-controlled oscillator (VCO) and two mixers. A differential cross-coupled oscillator is used to generate 24 GHz signals. Figure 4 shows a schematic representation of the VCO. The VCO core circuit uses a one
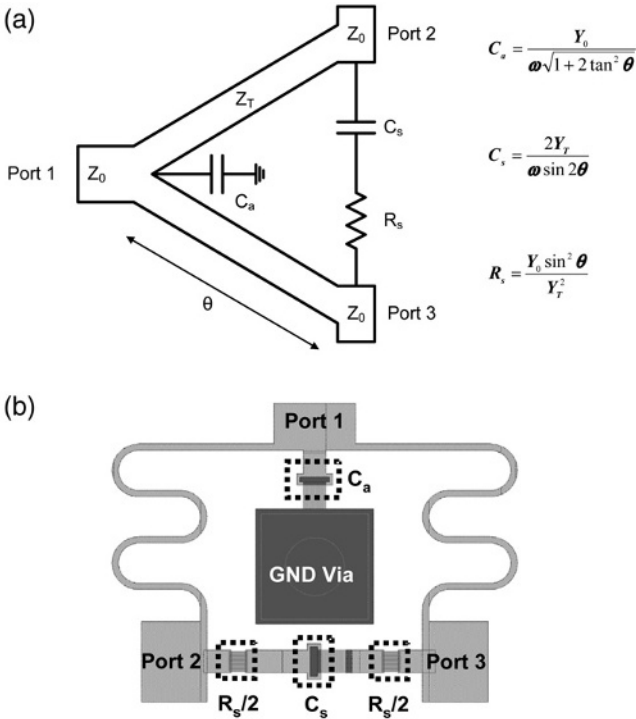
Figure 3. Improved lumped-distributed Wilkinson combiner: (a) topology and (b) designed layout.
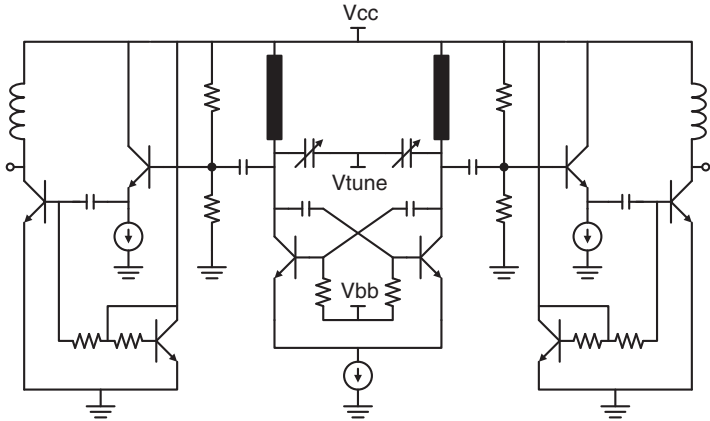

Figure 4. Schematic representation of a differential cross-coupled VCO.

finger $1 \times 4\,\mu m^2$ HBT. This device has a cutoff frequency (f_T) of 50 GHz and a maximum oscillation frequency (f_{MAX}) of 110 GHz. The turn-on voltage of an HBT is 1.21 V. The LC tank of the VCO is implemented with a microstrip line inductor and an MIM capacitor. Because the microstrip line inductors have a higher-quality factor and a higher
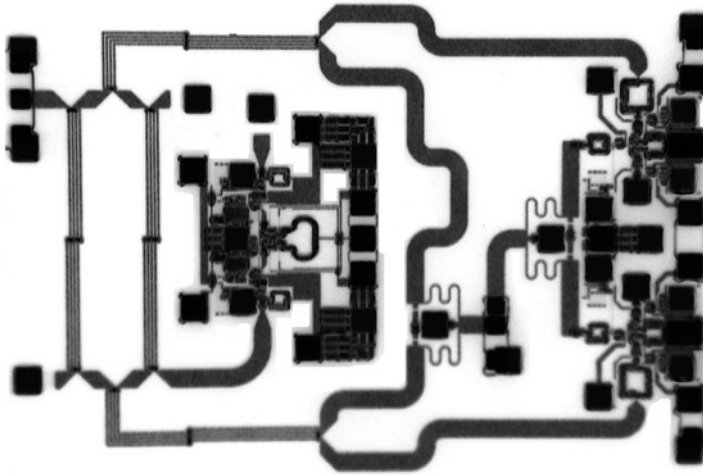
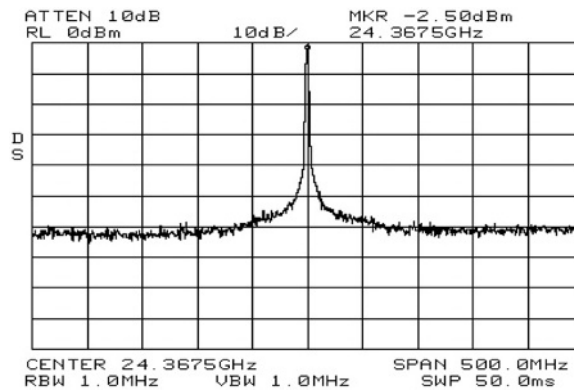Figure 5. Photograph of the front-end MMIC of a quadrature radar.

Figure 6. Measured output spectrum of a differential cross-coupled VCO.

self-resonant frequency than on-chip spiral inductors in a millimetre-wave band, a low-phase noise performance can be achieved. The base–collector junction capacitance of the HBT is used as a varactor for the frequency tuning, and a single balanced mixer is used to downconvert the signal.

2.5. *Measurement results*

Figure 5 shows microphotographs of the quadrature Doppler radar front-end IC. The chip is $3 \times 2 \, mm^2$. The fabricated VCO was tested with GS probes on a Cascade probe station. Figure 6 shows an output spectrum of the fabricated VCO; it has clear spectral purity without any other spurious signals. All the losses of the microprobe, cable and connectors

Table 2. Summary of the fabricated VCO.

Oscillation frequency	24.36–24.61 GHz
Peak output power	1.33 dBm
Phase noise	−94 dBc/Hz @ 1 MHz
Tuning range	250 MHz
Core DC bias	4.5 V (8 mA)
Chip size	$0.95 \times 1.2 \, mm^2$

Table 3. Summary of the fabricated mixer.

Conversion gain	11 dB
LO to IF, RF isolation	17.3 dB, 17.4 dB
P1 dB	−3.5 dBm
DC bias	5 V (23.2 mA)
Chip size	$0.46 \times 0.8 \, mm^2$

are about 3 dB at the K-band. Hence, we compensated for the measurement loss when calculating the output power of the VCO. A free running oscillation frequency of 24.36 GHz was achieved with the supply of 4.5 V and 8 mA. It provides an output power of 0.5 dBm. The frequency tuning range reaches 250 MHz from a range of 24.36 to 24.61 GHz as the varactor voltage varies from 4 to 0 V. The phase noise is −94 dBc/Hz at a 1 MHz offset from the operating frequency. Table 2 presents the measurement results of the fabricated VCO and Table 3 the results of the mixer.

3. Fabrication of the quadrature radar module and the measurement results

As shown in Figure 7, the quadrature radar front-end IC with decoupling SMD capacitors is mounted on an RO3003 printed circuit board. A 2×1 patch array antenna was designed on the same printed circuit board with a 2.5D EM simulator (Kim et al. 2007). The return loss is −27.4 dB at 24 GHz and the bandwidth (−10 dB) is approximately 1.5 GHz. The baseband outputs of the front-end module were filtered with Stanford Research System model SR560 LNAs with a 0.03 Hz high-pass analogue filter and a 10 Hz low-pass analogue filter, each with a 20 dB/decade slope and a gain of 26 dB. The preconditioned quadrature output signals were converted to digital data with a PCMCIA-type NI DAQ 6024E card, which has an input resolution of 12 bits. The data collected with the DAQ card were processed with a 3 Hz low-pass digital filter and displayed with a signal-processing programme developed with LabVIEW 7.0. We tested the quadrature mixing of the radar front-end by measuring the velocity of the moving metal plate ($0.09 \, m^2$) mounted on a rail that can only move back and forth along one axis at a fixed speed. The metal plate is about 1.7 m away from the radar. As shown in Figure 8, clean quadrature Doppler signals can be obtained. The phase of the Q-channel signal is retarded and advanced with respect to that of the I-channel as the target moves back and forth from the radar.
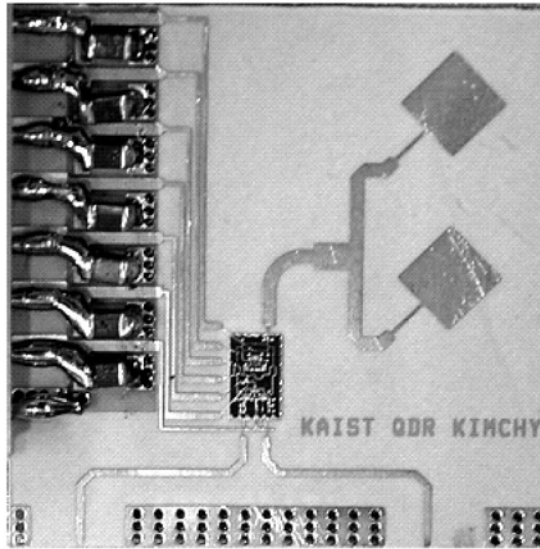
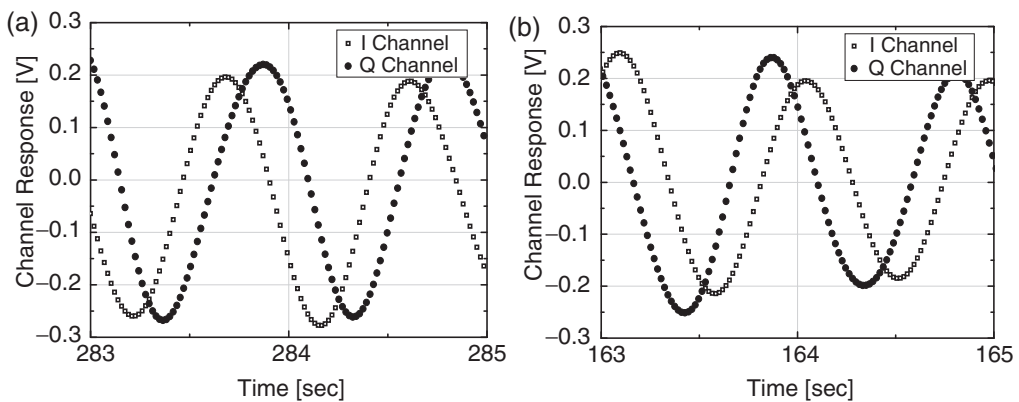Figure 7. Photograph of the fabricated quadrature radar front-end module.

Figure 8. Measured channel responses: (a) when the target moves away from the sensor and (b) when the target moves towards the sensor.

In addition, it is possible to obtain the target speed from the above results by calculating the Doppler frequency. The Doppler frequency shift is 1.23 Hz. The calculated speed of the target from the Doppler frequency is 7.53 mm/s. Target speeds of 2.5–10 mm/s were also measured. Table 4 presents the results. The direction and the speed of the moving target can be detected by the quadrature radar sensor.

4. Conclusion

A compact single-chip 24 GHz quadrature Doppler radar front-end module is developed using the MMIC technology for velocity and displacement measurements. A Tx leakage

Table 4. Doppler shift measurement.

Rail speed (mm/s)	Measured Doppler shift (Hz)	Measured speed by Doppler (mm/s)
2.5	0.411	2.5
5	0.823	5.01
7.5	1.23	7.53
10	1.647	10.04

canceller was implemented with simple passive devices: namely four Lange couplers, a 90° microstrip delay line and a Wilkinson combiner. Two of the Lange couplers (couplers 2 and 3), which are shown in Figure 2(b), are bent to reduce the size. The bent Lange coupler has a lower coupling factor due to the higher odd mode impedance in the bent area. A compact Wilkinson combiner topology is also used to reduce the size. Quadrature radar front-end module about 75% smaller than a similar module using PCB hybrid technology is developed. The quadrature radar module can measure speeds as low as 2.5 mm/s, which corresponds to a 0.41 Hz Doppler shift. Because of its quadrature topology, it can also detect signs of the Doppler shift.

Acknowledgements

References

Chen, Y., Hsieh, H., and Lu, L. (2008), 'A 24-GHz Receiver Frontend with an LO Signal Generator in 0.18-μm CMOS', *IEEE Transactions on Microwave Theory and Techniques*, 56, 1043–1051.

Chirala, M.K., and Nguyen, C. (2006), 'Multilayer Design Techniques for Extremely Miniaturized CMOS Microwave and Millimeter-wave Distributed Passive Circuits', *IEEE Transactions on Microwave Theory and Techniques*, 54, 4218–4224.

Chongcheawchamnan, M., Siripon, N., and Robertson, I.D. (2001), 'Design and Performance of Improved Lumped-distributed Wilkinson Divider Topology', *Electronics Letters*, 37, 501–503.

Droitcour, A.D., Lubecke, O.B., Lubecke, V.M., Lin, J., and Kovacs, G. (2004), 'Range Correlation and I/Q Performance Benefits in Single-chip Silicon Doppler Radars for Noncontact Cardiopulmonary Monitoring', *IEEE Transactions on Microwave Theory and Techniques*, 52, 838–848.

Ho, T., and Chung, S. (2010), 'Design and Measurement of a Doppler Radar with New Quadrature Hybrid Mixer for Vehicle Applications', *IEEE Transactions on Microwave Theory and Techniques*, 58, 1–8.

Hsieh, H., Liao, Y., and Lu, L. (2007), 'A Compact Quadrature Hybrid MMIC Using CMOS Active Inductors', *IEEE Transactions on Microwave Theory and Techniques*, 55, 1098–1104.

Kim, C.-Y., Kim, J.-G., and Hong, S. (2007), 'A Quadrature Radar Topology with Tx Leakage Canceller for 24 GHz Radar Applications', *IEEE Transactions on Microwave Theory and Techniques*, 55, 1438–1444.

Kim, S., and Nguyen, C. (2003), 'A Displacement Measurement Technique Using Millimeter-wave Interferometry', *IEEE Transactions on Microwave Theory and Techniques*, 51, 1724–1728.

Kim, S., and Nguyen, C. (2004), 'On the Development of a Multifunction Millimeter-wave Sensor for Displacement Sensing and Low-velocity Measurement', *IEEE Transactions on Microwave Theory and Techniques*, 52, 2503–2512.

Klotz, M., and Rohling, H. (2001), 'A 24 GHz Short-range Radar Network for Automotive Application', in *Proceedings of the IEEE Radar Conference*, pp. 115–119.

Meinel, H.H. (1995), 'Commercial Applications of Millimeter Waves History, Present Status, and Future Trends', *IEEE Transactions on Microwave Theory and Techniques*, 43, 1639–1653.

Nicolson, S.T., Chevalier, P., Sautreuil, B., and Voinigescu, S.P. (2008), 'Single-chip W-band SiGe HBT Transceivers and Receivers for Doppler Radar and Millimeter-Wave Imaging', *IEEE Journal of Solid-State Circuits*, 43, 2206–2217.

Russel, M.E., Drubin, C.A., Marinilli, A.S., Woodington, W.G., and Del Checcolo, M.J. (2002), 'Integrated Automotive Sensors', *IEEE Transactions on Microwave Theory and Techniques*, 45, 674–677.

Skolnik, M.I. (1980), *Introduction to Radar Systems* (2nd ed.), New York: McGraw-Hill Book Company.